Environ. Sci. Technol. **2002**, *36,* 254−262

Dissolved Gases as Partitioning Tracers for Determination of Hydrogeological Parameters

VIJAY M. VULAVA,* EVAN B. PERRY, CHRISTOPHER S. ROMANEK, AND JOHN C. SEAMAN

Advanced Analytical Center for Environmental Sciences, Savannah River Ecology Laboratory, The University of Georgia, Drawer E, Aiken, South Carolina 29802

In this study, dissolved Kr and SF_6 gases were used to determine various hydrogeological parameters of laboratory columns under water-saturated and partially saturated conditions as a function of the flow velocity. The dissolved gases behaved conservatively in saturated columns but were significantly retarded in unsaturated conditions as a direct function of the Henry's law constant (K_H) and the ratio of column pore spaces filled with air and water (V_g/V_w). Lower aqueous diffusion coefficients for SF_6 compared to that for Kr also resulted in significant rate-limited mass transport across gas−water interface. This effect was exacerbated at higher flow velocities as was indicated by the asymmetric shape of breakthrough curves, more so in the case of SF_6. A nonequilibrium advective-dispersive transport model accurately described tracer breakthrough and was used to estimate parameters such as final V_g/V_w under partially saturated conditions and partitioning rates. Internally consistent model results were obtained for both dissolved gases despite the wide range in physical properties (e.g., K_H and aqueous diffusion coefficients), suggesting that dissolved Kr and SF_6 may be used in conjunction to delineate and validate aquifer characteristics simultaneously from a single pulse injection of the tracer.

1. Introduction

Tracers are typically injected into groundwater to obtain information concerning the direction and/or velocity of water movement in aquifers and the potential transport of contaminants. Ideally, such tracers track the movement of groundwater through porous media without altering the physical or chemical conditions of the aquifer. As such, they should be (1) intrinsically stable and nonreactive with porous media, (2) present in extremely low background concentration, (3) detectable at low concentration, and (4) similar to native groundwater in density.

Inorganic and organic anions such as Cl^-, Br^-, and fluorinated benzoic acid derivatives (e.g., pentafluorobenzoic acid) are typically considered "conservative" or nonreactive under most conditions (*1*−*3*), but under certain conditions they exhibit significant retardation in field (*4*) and laboratory studies (*5*−*11*). Seaman et al. (*6*, *8*, *12*) showed that most anionic tracers are highly retarded in aquifer sediments of the Atlantic Coastal Plain because of sorption onto variably charged Fe-oxides. In these studies, water enriched with tritium (^3H) was used to confirm the retardation of anionic tracers. However, health and regulatory concerns make it difficult to use radioactive tracers in most field applications, and hence other solutes are needed for use as conservative tracers.

Dissolved gases may be used to determine parameters such as groundwater velocity, aquifer porosity, and dispersivity in site-characterization studies. Nonreactive and nonpolar gases do not react with most porous media during transport nor do they influence significantly the physicochemical properties of groundwater. They are safe to use in porous media sensitive to changes in solution chemistry or ionic strength. Contrary to many ionic tracers, dissolved gases such as helium (He), neon (Ne), krypton (Kr), and sulfur hexafluoride (SF_6) can be measured analytically over several orders of magnitude. Despite these advantages, relatively few studies have demonstrated the use of dissolved gases as conservative hydrologic tracers (*13*−*20*). Recent attention has focused primarily on the use of dissolved anthropogenic gases, such as SF_6 and chlorofluorocarbons (CFC), to determine gas-transfer rates between atmosphere and groundwater (*21*−*25*). Because the atmospheric concentration of these gases has increased, these gases have also been used to date groundwater ages (*26*, *27*).

The widespread use of dissolved gases as tracers has been hampered because of perceived difficulties in deploying and recovering the tracer in the field. In addition, factors such as temperature differences between the groundwater and tracer solution and the potential exsolution of gases have limited their use. With the increasing sophistication of analytical techniques, quantitative recovery and analysis of dissolved gases has become considerably simpler and more accurate. Sample extraction via sparging and sonication followed by headspace analysis using gas chromatography coupled with an electron capture detector or a quadrupole mass spectrometer provides a superior analytical tool for the analysis of most gases that have some relevance as tracers (*13*, *28*−*30*). These techniques yield extremely low detection limits; hence, some tracers may be injected at relatively low concentration and detected long distances from the point of origin.

Sulfur hexafluoride, an anthropogenic gas used in electric insulating equipment (*27*), is nonpolar, inert, and has an extremely low ambient background concentration (<3 pptv) and slight aqueous solubility (~35 mg/L, 1 atm pure gas at 25 °C). In some laboratory column and field applications, SF_6 has been shown to exhibit transport behavior similar to that of solute tracers such as Cl^- and Br^- (*17*, *19*, *31*). However, SF_6 was found to be retarded in the presence of air pockets or residual nonaqueous phase liquids in the porous media (*14*, *19*, *31*, *32*). Noble gases, such as He (*15*, *20*, *33*) and Kr (*13*, *34*), have also been used as tracers in both laboratory and field tracer studies with mixed results. Both gases are relatively inert and naturally present in low concentration in groundwaters.

Table 1 lists relevant properties of Kr and SF_6 for comparison. The most relevant property for tracer application is the Henry's law constant (K_H, dimensionless) which relates aqueous and air phase concentrations of a gas (*35*)

$$K_H = \frac{c_g}{c_w} \quad (1)$$

* Corresponding author phone: (865)974-9976; fax: (865)974-2368; e-mail: vulava@utk.edu. Present address: Department of Geological Sciences, The University of Tennessee, 1412 Circle Drive, Knoxville, TN 37996-1410.

10.1021/es0107024 CCC: $22.00
Published on Web 12/12/2001

TABLE 1. Relevant Chemical Properties and Measurement Conditions for SF_6 and Kr

property	SF_6	Kr
molecular weight (g/mol)	146.06	83.8
Henry's law constant[a] (25 °C)	170.4	18.0
solubility[b] (mg/L at 1 atm)	35.2	234
diffusion coeff in water[c] (cm^2/s)	$1.20 \cdot 10^{-5}$	$1.84 \cdot 10^{-5}$
diffusion coeff in air[d] (cm^2/s)	$6.1 \cdot 10^{-2}$	$8.7 \cdot 10^{-2}$
atmospheric concn[e] (pptv)	~3	$1.14 \cdot 10^{6}$
background aq concn[f] (mg/L)	$1.76 \cdot 10^{-8}$	$2.7 \cdot 10^{-4}$
gas chromatographic detector	electron capture detector	mass spectrometer
column packing	DB-5/DB-VRX	Carboxen-1010 PLOT
carrier gas	He	He
detection limit[g] (mol)	$6.8 \cdot 10^{-12}$	$1.2 \cdot 10^{-11}$

[a] Reference (*51*). [b] Wilson and Mackay (*31*) at 24 °C and Davis et al. (*28*) at 20 °C for SF_6 and Kr respectively; estimated to be 35.03 and 209.36 mg/L, respectively, using K_H, at 25 °C. [c] Wilson and Mackay (*31*) and Jahne et al. (*52*) for SF_6 and Kr, respectively, estimated to be $0.78 \cdot 10^{-5}$ and $1.2 \cdot 10^{-5}$ for SF_6 and Kr, respectively, according to an empirical relation $2.7 \cdot 10^{-4}/m^{0.71}$, where m is the molecular mass of the chemical (*35*). [d] Estimated using an empirical relation $1.55/m^{0.65}$, where m is the molecular mass of the chemical (*35*). [e] Butler et al. (*53*) and Gluekauf and Kitt (*54*) for SF_6 and Kr, respectively. [f] Estimated from K_H and atmospheric concentration. [g] Present study.

where c_g and c_w are the gaseous and aqueous phase concentrations (ML^{-3}), respectively. The value of K_H is greater than one for both Kr and SF_6, indicating they are hydrophobic and preferentially partition into pore spaces that are occupied by gas or other nonpolar compounds (e.g., organic solvents). With respect to gas-filled void space in partially saturated media, dissolved gases display increased retardation due to partitioning at the gas−water interface. Retardation can also be attributed to preferential "sorption" onto surfaces in some heterogeneous materials (e.g., organic matter, porous sediments, etc.) (*17*, *20*). With an understanding of this behavior, partitioning tracers in combination with nonpartitioning tracers can provide additional physical and chemical characterization of groundwater systems than nonpartitioning tracers alone. Such information may be vital to the successful application of gas venting or sparging operations in the remediation of subsurface porous media contaminated with organic solvents.

The primary objective of this study was to evaluate the combined use of dissolved Kr and SF_6 as partitioning tracers in partially water-saturated porous media to determine hydrogeological parameters (e.g., volume of gas-filled void spaces, partitioning rates, etc.) in model flow systems. Despite the large differences in physicochemical properties, both dissolved Kr and SF_6 will be shown to provide internally consistent results suggesting they can be used with confidence to model hydraulic properties and aquifer characteristics that are difficult to assess by other methods.

2. Materials and Methods

2.1. Preparation of Tracer Water. Tracer solutions used in all experiments were prepared by dissolving Kr (99.97% pure, BOC Gases) and SF_6 (99.99% pure, Scott Specialty Gases) gas in deionized water enriched in tritium (^3H). SF_6 (g) was bubbled into a 2 L Pyrex bottle containing about 1.5 L of water for ~30 s until all headspace in the bottle was flushed with the tracer gas. The bottle was sealed with a Teflon cap containing ports, a recirculating pump was attached, and the headspace SF_6 was cycled through the water to establish equilibrium between the liquid and the gas phase. This procedure was then repeated with Kr gas. Bubbling in this manner provided a tracer solution containing ~130 mg/L Kr and ~1 mg/L SF_6.

2.2. Dynamic Flow Experiments. Well-graded 20−30 mesh Ottawa standard sand (>98% quartz, Fisher) was uniformly packed into either 2.5 or 1.0 cm i.d., 30 cm long glass columns (Kontes) that were tightly capped with Teflon end-pieces (wall thickness >0.5 cm) and stainless steel or brass valves at each end. The sand medium had an average bulk density of 1.75 (±0.04) g/cm^3 and a porosity of 0.36 (±0.01). Stainless steel and/or copper tubing (1/16 in. i.d.) was used to plumb the entire experimental setup because of its low adsorptive capacity.

Dry packed columns were flushed with CO_2 gas for ~30 min to replace air in the void space. Carbon dioxide (K_H = 1.2) was used because it dissolves more readily in water than air, facilitating saturation when water was introduced into the column. The column was saturated with liquid by pumping deionized water from below in an upflow direction. Close examination of saturated columns did not reveal any visible gas bubbles in the sand matrix.

Tracer solution containing dissolved Kr and SF_6 was then injected into the column at a constant flow rate, and column effluent (2 mL sample size) was collected with a generic liquid fraction collector (Foxy, Isco Inc.) in 10 mL gas chromatography headspace glass vials (Kimble). The vials were immediately capped with septa (Agilent) and sealed using aluminum crimps (Kimble) to minimize loss of dissolved gases. Dissolved gas concentrations obtained in this fashion were comparable (<2% lower) with the concentrations for samples collected using a Gilson Liquid Handler 215 (Gilson Inc.) fraction collector which injects samples directly into presealed vials. However, the Gilson fraction collector was unable to collect uniform sized samples due to excessive back pressure at flow rates greater than 0.2 mL/min caused by the small-bore syringe at the delivery point. The sample masses collected were consistent throughout every experiment at all flow rates; based on these criteria, losses in dissolved gas concentrations were assumed to be <2% for all samples collected in each experiment. Influent tracer solution was sampled at the beginning and end of each experiment in a similar fashion for comparison with the column effluent. Measured effluent tracer concentrations (C) were normalized to the influent concentration (C_0), so absolute dissolved concentrations were not required for data analyses. Several pore volumes of the tracer-free water were injected after the introduction of a long pulse of tracer water (see Table 2) through the column.

In a manner similar to that used by Fry et al. (*17*) and Donaldson et al. (*36*), gas-filled void space (V_g/V_w), expressed as percent of the initial pore volume of the water-saturated column (V_w) displaced by air (V_g), was introduced into the saturated column by draining some water from the bottom. The column was then flushed with deionized water for several pore volumes (>5) to stabilize the newly created gas-filled void space. Note that the flushing of the column with water does not completely resaturate the column to the predrain levels due capillary forces between the pores. The partially saturated column was assumed to have reached steady state when no appreciable change in the column mass (±0.1%)

TABLE 2. Relevant Experimental and Estimated Hydrological Parameters[a]

exp.	tracer	column i.d., cm	pulse, PV	velocity, cm/s	recovery, %	*P*	*D*, cm^2/s	α, s^{-1}
1	^3H_2O	2.5	1	0.04	100	400	0.003	
	SF_6			0.04				
	Kr			0.04				
2	^3H_2O	2.5	5.5	0.04	100	400	0.003	
	SF_6			0.04	29.1			$3.50 \cdot 10^{-4}$
	Kr			0.04	98.4			$2.33 \cdot 10^{-3}$
3	^3H_2O	2.5	6.5	0.04	100	400	0.003	
	SF_6			0.04	25.6			$7.19 \cdot 10^{-4}$
	Kr			0.04	98.7			$4.82 \cdot 10^{-3}$
4	^3H_2O	1.0	25	0.01	100	300	0.001	
	SF_6			0.01	63.9			$9.31 \cdot 10^{-5}$
	Kr			0.01	98.7			$8.49 \cdot 10^{-4}$
5	^3H_2O	1.0	20	0.08	100	300	0.008	
	SF_6			0.08	63.4			$4.24 \cdot 10^{-4}$
	Kr			0.08	96			$4.39 \cdot 10^{-3}$
6	^3H_2O	1.0	19.4	0.24	100	300	0.023	
	SF_6			0.24	83.8			$1.17 \cdot 10^{-3}$
	Kr			0.24	98.7			$1.31 \cdot 10^{-2}$

[a] Pulse indicates the amount of tracer water injected (in pore volumes, PV) into the column. Recovery was calculated by integrating area under the breakthrough curves. Dispersion coefficient (*D*) and Péclet number (*P*) were determined based on ^3H_2O breakthrough and were fixed for estimating *R*, V_g/V_w, and α values. The kinetic rate coefficient (α) for dissolved SF_6 and Kr are calculated from eq 7a.

was observed. This was determined by repeated gravimetric measurements of the column setup after gas-filled void space was introduced (i.e., quasi steady-state conditions). Tracer experiments were conducted on columns with different volumes of gas-filled void space (see Table 2). We recognize that the spatial distribution of gas bubbles may influence the mass transport characteristics; such characterization is beyond the scope of this study.

Dissolved gas breakthrough curves were compared to breakthrough curves for water enriched in ^3H (referred to hereafter as ^3H_2O) to calibrate the flow of tracers against the actual movement of water through the column. The dispersion coefficient (D, L^2T^{-1}) was determined by fitting the ^3H_2O breakthrough curve to an equilibrium advective-dispersive transport equation (*37*).

2.3. Analytical Measurements. Due to the distinct physical properties of Kr and SF_6, different gas chromatographic (GC) techniques were required to analyze each gas. Dissolved gases in the sample vials were allowed to equilibrate with the headspace by vigorously shaking for 30 s. The headspace was then subsampled for Kr and SF_6 followed by analysis of the water for tritium content.

Gas standards for calibration were prepared using a vacuum line to mix pure gases in lecture bottles at different pressures. Kr and SF_6 calibration curves were constructed by sampling known amounts of calibration gas injected into 10 mL headspace vials that were filled with air.

2.3.1. Kr Analysis. A Hewlett-Packard (HP) 5890 gas chromatograph (GC) equipped with a 5970 Mass Selective Detector (MSD) was used for Kr analysis. Equilibrated vial headspace was sampled with a 10 μL gastight syringe and injected directly onto the GC column. A Supelco Carboxen 1010 plot column (30 m × 0.53 mm) was used to separate Kr and Ar from air when the GC was operated isothermally at 155 °C. The MSD was operated in selected ion monitoring (SIM) mode, where the masses of the six stable isotopes of Kr ($^{78,80,82,83,84,86}Kr$) were measured sequentially. Additionally, the three stable isotopes of Ar ($^{36,38,40}Ar$) were analyzed to serve as an internal standard. The peak area of Kr was divided by that of Ar to minimize analytical uncertainty caused by factors such as inconsistencies in injection volume, changes in room temperature during analysis, and cleanliness of the MSD source (*38*). Because headspace in the vials contained a fixed background of Ar (~9500 mg/L in air) at significantly

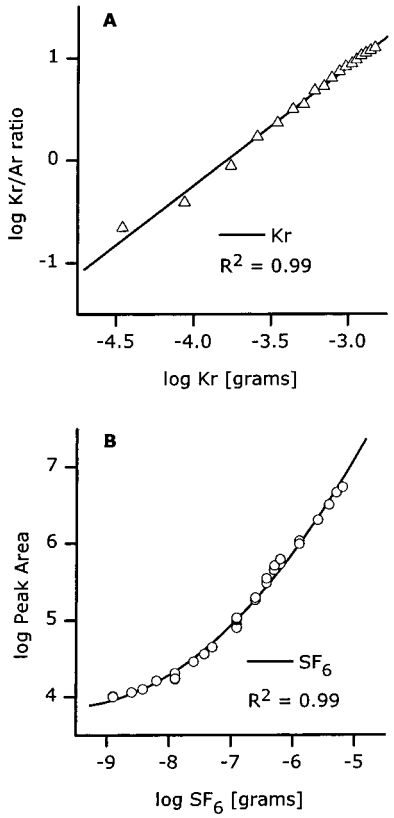

FIGURE 1. Calibration curves for Kr (△) and SF_6 (○) measured with GC-mass selective detector and GC-electron capture detector, respectively.

greater concentration than ambient Kr (>100×), this method of analysis permitted the precise measurement of Kr concentration over a wide range of concentrations (Figure 1).

2.3.2. SF_6 Analysis. A second HP 5890 GC equipped with an Electron Capture Detector (ECD) was used for SF_6 analysis. A DB-5 (30 m × 0.25 mm, isothermal at 32 °C) or DB-VRX (60 m × 0.25 mm, isothermal at 200 °C) capillary column was used for separation of SF_6 from air in the equilibrated headspace of samples. Samples were introduced into the GC with an HP 7694 auto headspace sampler. The detector

TABLE 3. Retardation (R) and V_g/V_w Values Estimated Using Various Methods[a]

		start of exp.[b]		end of exp.[b]		model[c]		mass balance[c]		time moments[c]	
exp.	tracer	V_g/V_w	R	V_g/V_w	R	R	V_g/V_w	R	V_g/V_w	R	V_g/V_w
1	^3H_2O	0		0		1		1.0		1.0	
	SF_6					1.1	0.06	1.1	0.1	1.0	0.0
	Kr					1	0.0	1.0	0.2	1.0	0.2
2	^3H_2O	3.9		6.3		1		1.0		1.0	
	SF_6		7.6		11.7	11.9	6.4	8.6	4.5	1.3	0.2
	Kr		1.7		2.1	2.2	6.7	2.3	7.5	2.4	7.9
3	^3H_2O	8.1		8.8		1		1.0		1.1	
	SF_6		14.8		16.0	13.4	7.3	10.6	5.6	2.6	0.9
	Kr		2.5		2.6	3	11.1	3.0	11.4	3.0	11.3
4	^3H_2O	1.0		3.1		1				1.1	
	SF_6		2.7		6.3	7.3	3.7	7.0	3.5	5.2	2.5
	Kr		1.2		1.6	1.4	2.2	1.3	1.7	1.5	2.6
5	^3H_2O	2.6		4.9		1				1.0	
	SF_6		5.4		9.3	7.5	3.8	7.1	3.6	5.0	2.4
	Kr		1.5		1.9	1.8	4.4	1.9	4.8	2.2	6.6
6	^3H_2O	2.2		3.5		1				1.1	
	SF_6		4.7		7.0	5.7	2.8	5.2	2.5	3.4	1.4
	Kr		1.4		1.6	1.6	3.3	1.8	4.4	1.7	4.1

[a] Gas-filled void space (V_g/V_w) is expressed as percent of the initial pore volume of the water-saturated column (V_w) displaced by air (V_g). [b] The hypothetical R values were estimated using eq 4 and the measured V_g/V_w at the start and end of the experiments. These V_g/V_w values were measured gravimetrically both before the tracer injection and at the end of the experiment. [c] The V_g/V_w values were estimated by fitting the breakthrough curves to the advective-dispersive model (eq 5), by mass balance method (eq 2), and by time moment method (eq 3).

provided a nonlinear but quantifiable calibration curve over 4 orders of magnitude (Figure 1). This nonlinear behavior has been reported previously for SF_6 measurement over a typical working range of concentrations for ECD analysis (*39*). A second-order polynomial regression was used to fit the detector response over this working range.

2.3.3. ^3H_2O Analysis. One or 2 mL of effluent was mixed with 10 mL of scintillation cocktail and counted for 20 min in a liquid scintillation counter (Minaxi Tri-Carb 4000, Packard Instrument Co.). Breakthrough estimates were based on the relative counts per minute for known amounts of the inlet tracer solution. A detection limit of ~2.5 pCi/mL (representing ~2% of the inlet ^3H_2O concentration) was typically achieved with this technique.

3. Results and Discussion

Tracer breakthrough curves were recorded following the injection of short pulses of the tracer solution into saturated or partially saturated columns. From the measured breakthrough curves for the tracers, retardation factors were estimated from the mass balance analysis of the step increase in influent concentration (*40*). The retardation was estimated according to the equation

$$R = \frac{\int_0^{C/C_0=1} (1 - C/C_0)_p dT}{\int_0^{C/C_0=1} (1 - C/C_0)_{np} dT} \quad (2)$$

where R is the retardation factor (dimensionless), C/C_0 denotes reduced concentration (ratio of effluent and influent tracer concentration, dimensionless), T is the number of pore volumes of solution passed through the column (dimensionless), and subscripts p and np denote partitioning (dissolved Kr and SF_6) and nonpartitioning (^3H_2O) tracers, respectively. Values for R are reported in Table 3 for each experiment.

Alternatively, R values were estimated using time moments for a simple step increase in influent tracer concentration as a complete breakthrough curve was not obtained in all cases. We adopted a relatively simple time moment method from Yu et al. (*41*) for estimating R. According to this method, the mean breakthrough time (R) in case of a step input is

$$R = \frac{\int_0^{C/C_0=1} T dC/C_0}{\int_0^{C/C_0=1} dC/C_0} \quad (3)$$

Note that $\int_0^{C/C_0=1} dC/C_0 = 1$ for a step increase. In both methods R values will be underestimated when the effluent concentration does not reach the influent concentration (compare R values from different methods in Table 3).

When one pore volume of tracer solution (Kr and SF_6 gases dissolved in ^3H_2O) was injected into a completely water-saturated column (exp. 1 in Table 2), all three tracers eluted almost simultaneously (Figure 2a). Under saturated conditions C/C_0 reached unity at one pore volume for Kr and ^3H_2O indicating that the tracers behaved conservatively, with little dispersion. However C/C_0 for SF_6 did not reach unity, which suggested the column may have contained an extremely small volume of gas-filled void space. Due to its extremely high K_H value (Table 1 and eq 1), SF_6 is very likely to partition even into the smallest of gas-filled void spaces. Sorption of SF_6 to the sand and or diffusion into sand grains was ruled out based on previous published results (*16*, *31*). A small amount of SF_6 may also have been lost during sampling as it is more volatile compared to Kr. Finally a small percent may have diffused into Teflon end pieces.

Sanford et al. (*15*) conducted similar experiments using dissolved He as a tracer in a water-saturated column containing fractured shale saprolite. They observed that He eluted after Br^- and attributed this to the preferential diffusion of He into the matrix based on a comparison of molecular diffusion coefficients. They also reported difficulty in attaining complete water saturation in their laboratory columns; these observations may be reconciled by the presence of microscopic gas-filled void spaces as He has a K_H value (108 at 25 °C) comparable to that of SF_6 (170 see Table 1). The inability to achieve complete saturation in such columns may only be observable when employing highly volatile dissolved gases as tracers, assuming that there are no other perceivable losses.

3.1. Influence of Gas-Filled Void Spaces. Long pulses (5−6 pore volumes) of tracer solution were injected in a set

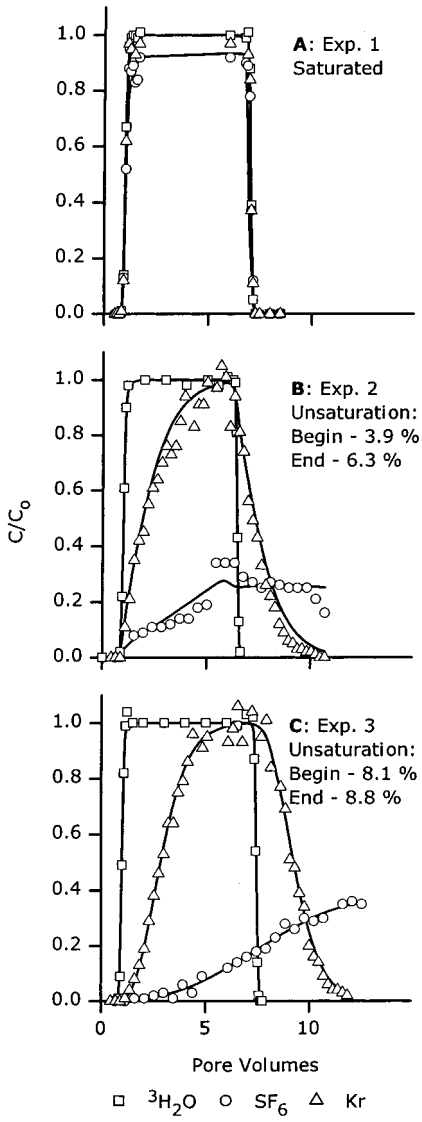

FIGURE 2. Breakthrough curves for ^3H_2O (□), SF_6 (○), and Kr (△) in saturated (A) and partially saturated sand columns with approximately 4% [B] and 8% [C] gas-filled void space. Flow velocity was 0.04 m/s for all experiments. Lines are model fits of the data, and symbols are the experimental data points. See Table 2 for description of exp. 1−3 (A−C, respectively).

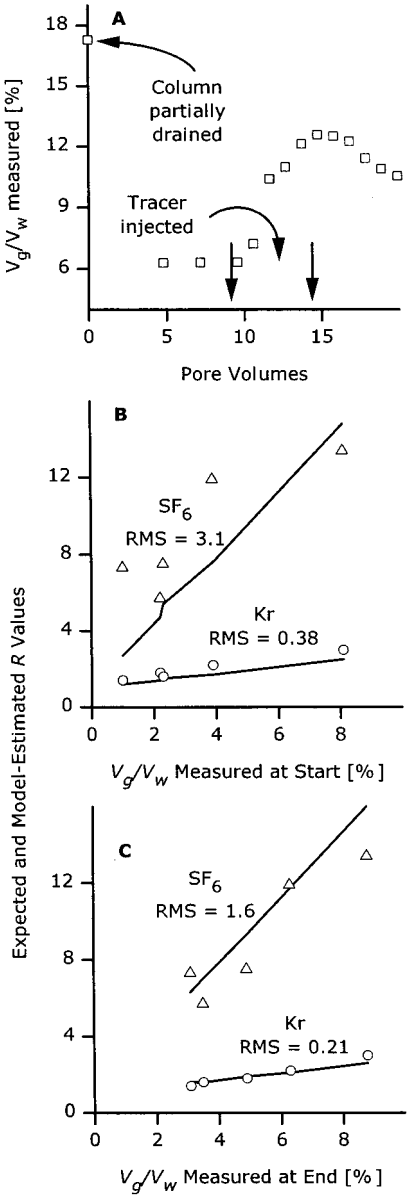

FIGURE 3. [A] Change in gravimetrically measured V_g/V_w values during injection of dissolved gas tracer through a partially saturated column. Note that initially several pore volumes of tracer-free water was injected into the partially saturated column until no change in V_g/V_w was observed. [B−C] Expected R values (lines) for SF_6 and Kr calculated using eq 4 for V_g/V_w values measured at the start (B) and end (C) of each experiment. These values are compared with R values (symbols) calculated using the model (△ for SF_6 and ○ for Kr) described in the text. Root mean square (RMS) of differences were calculated for each set of data between expected and model-estimated R values. See Table 3 for experimental data.

of column experiments under identical flow velocities but with different initial values of V_g/V_w (exp. 2−3 in Table 2). The resulting breakthrough curves indicated that Kr and SF_6 were retarded compared to ^3H_2O (Figure 2B,C). In all cases, the effluent Kr concentration reached the initial concentration (C_0) within a few pore volumes. However, the C/C_0 value for SF_6 barely reached 0.2. Mass balance calculations indicated that <30% of injected SF_6 was recovered as compared to nearly 100% recovery for Kr (Table 2). The presence of gas-filled void space within the column influenced the transport of dissolved SF_6 more than Kr. It is clear that by increasing V_g/V_w, R increased for both gases, while ^3H_2O remained unaffected (Table 3).

Following the injection of tracer solution into partially saturated columns, final V_g values increased compared to initial values (Table 3). This indicated not only that the dissolved gases partitioned into gas-filled void space but also that the partitioning processes also displaced water from the column throughout the experiment (Figure 3A). While this increase was significant for small values of V_g/V_w, only a marginal increase was observed for higher values of V_g/V_w. Further examination indicated that V_g increased during tracer solution injection and then decreased when tracer-free water was flushed through the column. Similar results have been reported by Fry et al. and Donaldson et al. (*17*, *36*) for dissolved O_2 transport in sand columns. The increase in V_g may be attributed to differential rates at which the dissolved gases and the air present in void spaces diffused out of and into the mobile water phase. As a rule of thumb, the more hydrophobic the gas, the faster it diffuses out of the aqueous phase (*35*). SF_6 is relatively hydrophobic and hence diffused out of the aqueous phase into the air phase faster than air into water during initial equilibration processes. The relative rates of diffusion can also depend on factors such as the

gaseous and aqueous diffusion rates and the relative masses and/or initial concentrations of the constituents. This observation suggests that the partitioning of dissolved gases into the air pockets in the column had, in fact, not reached a true steady state. This condition is analogous to hysteresis commonly observed in case of chemisorption to environmental media.

Fry et al. (*17*) derived a retardation term for the transport of dissolved O_2 in terms of V_g/V_w and K_H as

$$R = 1 + K_H \frac{V_g}{V_w} \tag{4}$$

Assuming local equilibrium between the gaseous and aqueous phases, retardation is dependent on K_H and V_g/V_w. In the present study, R values increased for both dissolved gases as V_g/V_w increased from 4 to 8% (Figure 2 and Table 3). Jardine et al. (*33*) noted a similar phenomenon in experiments with dissolved He ($K_H = 108$ at 25 °C) and Ne ($K_H = 91$ at 25 °C) gas tracers in a fractured bedrock water table aquifer. They reported that Ne was detected earlier than He several meters from the injection well. We believe that the difference in retardation of these gases may be related to differences that control their K_H values (cf. eq 4).

Longer pulses of tracer solution were injected into three columns with similar initial V_g/V_w values (exp. 4−6 in Table 2) at different flow velocities (Figure 4). The tracers eluted in the same order as in exp. 2 and 3. Better mass recovery was achieved in this set of experiments in case of SF_6 (>65% recovered) due to relatively longer sampling times (cf. exp. 1−3).

3.2. Modeling of Transport. Equilibrium advective-dispersive transport equations have been used to accurately describe conservative tracer breakthrough curves (*42*). As shown above for our experiments, all tracers behaved nearly conservatively when the columns were completely saturated. However, a different approach is required for accurately modeling the advective transport of a tracer affected by partitioning between the aqueous and gaseous phase (*43*).

As mentioned above, Fry et al. (*17*) modeled transport of dissolved O_2 assuming that instantaneous equilibrium existed between water and trapped gas phases; however, their approach failed at relatively high values of V_g/V_w. Donaldson et al. (*36*) suggested that inadequate tracer residence time results in diffusion-limited transport of dissolved gas tracers across gas−water interface. Hence, a nonequilibrium approach would be more appropriate where kinetics of gas partitioning are important. The asymmetric shape of the breakthrough curves in our experiments, especially in the case of SF_6, is a clear indication of kinetically limited mass transfer (*42*). As this behavior was not observed for ^3H_2O, physical nonequilibrium (usually due to the presence of immobile pockets of water) can be ruled out.

A two-region/two-phase reactive transport equation, commonly applied to describe the movement of heavy metals or organic compounds in environmental porous media, was used to model the experimental data (*37*, *43*). The equation for steady-state mass transport of dissolved gases can be described as

$$V_g \frac{\partial c_g}{\partial t} + V_w \frac{\partial c_w}{\partial t} = V_w D \frac{\partial^2 c_w}{\partial x^2} - V_w \nu_w \frac{\partial c_w}{\partial_x} \tag{5}$$

where D is the dispersion coefficient (L^2T^{-1}), ν_w is the average pore water velocity (LT^{-1}), x is distance traveled (L), and t is time (T). To apply this equation to the current set of data it is implicitly assumed that gas-filled void space is uniformly distributed within the entire column. We recognize that this is not true, but, based on the modeling results, it will be shown that this approximation provides fairly accurate model results for the experimental data.

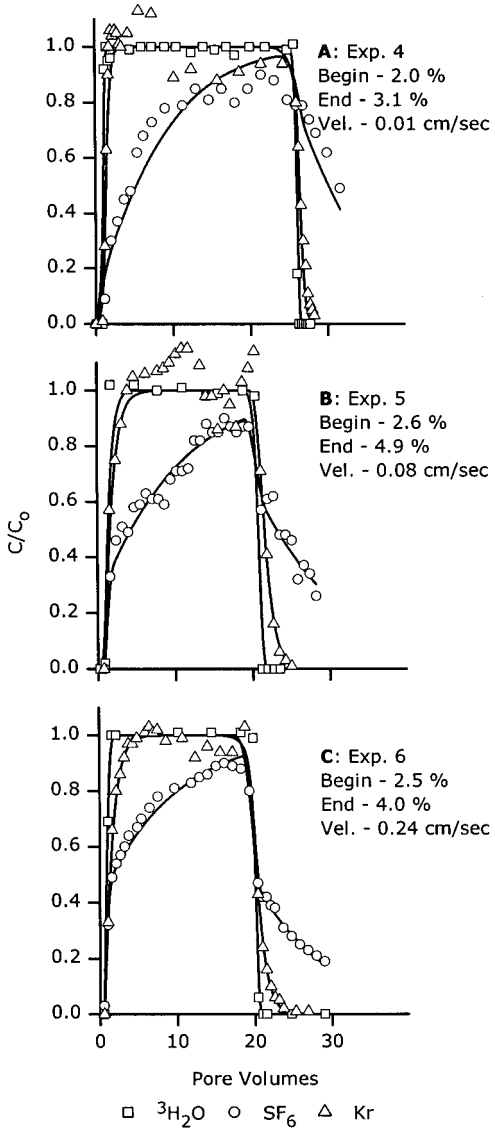

FIGURE 4. Breakthrough curves for ^3H_2O (□), SF_6 (○), and Kr (△) in partially saturated sand columns with approximately 3% gas-filled void spaces and at uniform flow velocities. Lines are model fits of the data and symbols are the experimental data points. See description of experimental data in Table 2 for exp. 4−6 for A−C, respectively.

The rate of change in dissolved gas tracer concentration across the gas−water interface is a function of the concentration gradient, the surface area of contact per unit volume of the gas bubbles, and the residence time of the tracer (*35*). Because dissolved gas partitioning is kinetically limited, it is best described by a first-order rate coefficient, α (T^{-1}). As the surface area of the gas bubbles was not measured directly, this term is assumed to be implicit in α. Hence, the rate of interfacial mass transfer is described as

$$\frac{\partial c_g}{\partial t} = \alpha(K_H c_w - c_g) \tag{6}$$

When $K_H c_w > c_g$, mass transfer will occur from the aqueous to gaseous phase. Equation 6 can be substituted into eq 5

and rewritten in a dimensionless form as

$$\frac{\partial C_w}{\partial T} + \omega(C_w - C_g) = \frac{1}{P}\frac{\partial^2 C_w}{\partial X^2} - \frac{\partial C_w}{\partial X} \quad (7)$$

The dimensionless parameters, C_w, C_g, T, X, P, and ω, are defined as

$$C_w = \frac{c_w}{c_w^\circ} \text{ and } C_g = \frac{c_g}{K_H c_w^\circ} \quad (7a)$$

$$T = \frac{\nu_w t}{L} \text{ and } X = \frac{x}{L} \quad (7b)$$

$$P = \frac{\nu_w L}{D} \quad (7c)$$

$$w = \frac{\alpha L(R-1)}{\nu_w} \quad (7d)$$

where c_w° is the concentration of the dissolved gas in the tracer solution at the inlet of the column, T is the ratio of cumulative volume of water pumped through the column to the pore volume, X is the distance (normalized with column length, L), P is a column parameter known as the Péclet number, and ω is a parameter that includes the rate coefficient (α) and retardation factor (R).

Analytical solutions for eq 7 were used for fitting breakthrough curves to estimate R, D, V_g/V_w, and α (*37*, *44*). First, ^3H_2O breakthrough curves were fitted to estimate P in each experiment. Because this value is a physical parameter for the column, P was fixed for subsequent modeling exercises of Kr and SF_6 breakthrough curves in each experiment. Values for R and ω were estimated by fitting the breakthrough curves for Kr and SF_6. Based on these estimates, V_g/V_w was estimated for each gas and compared with the measured value (eq 4); α was also calculated from ω to establish a relationship between α and parameters such as ν_w and V_g/V_w (eq 7d). In all cases, the estimated value of P from fitting ^3H_2O breakthrough curves was relatively large (Table 2), implying negligible dispersion effects in the column.

The expected R values for all experiments can be calculated using eq 4 and the V_g/V_w values measured at the beginning and end of the experiments. In all cases, the R values estimated by the model calculations compared favorably with the expected R values calculated with V_g/V_w values obtained at the end of all experiments (Figure 3B,C). This was ascertained from the reduction in the root-mean-square of differences (RMS $= \sqrt{\sum_{i=1}^{i=n}(R_{calc,i} - R_{est,i})^2}$) between the calculated and expected R values.

In describing the breakthrough curves for the saturated column (exp. 1, Table 2), both the equilibrium and nonequilibrium models faithfully predicted nearly piston-flow type transport (see Figure 2A). However, the nonequilibrium model predicted slight retardation in the case of SF_6 which is equivalent to the presence of 0.1% V_g/V_w in the column (eq 4). While this degree of partial saturation cannot be substantiated due to experimental error associated with the gravimetric analyses, it is consistent with the tendency of SF_6 to significantly partition into even the smallest percentage of gas-filled void space in the column. In addition, there may have been loss of more dissolved SF_6 compared to Kr during sampling due to higher K_H or greater relative diffusion into various potential sinks (e.g., Teflon end pieces).

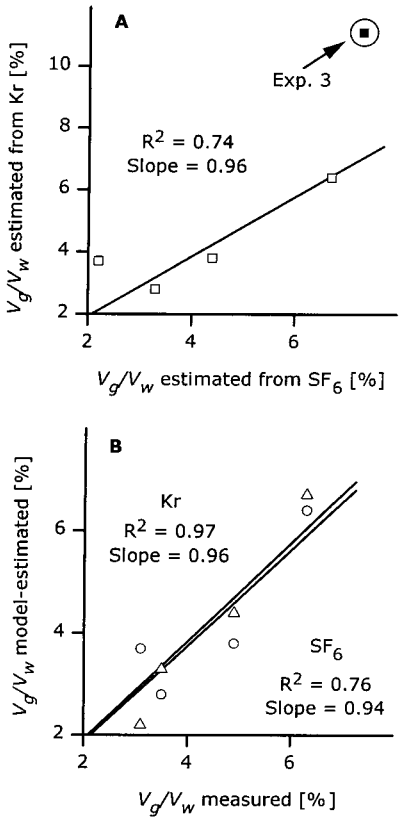

FIGURE 5. [A] Linear correlation of V_g/V_w from modeling of SF_6 and Kr breakthrough curves. The outlier is from exp. 3 (see Table 3) and has not been included in the fitting. [B] Linear correlation between gravimetrically measured V_g/V_w (at the end of the experiment) and model-estimated V_g/V_w for dissolved SF_6 (○) and Kr (△) (see Table 3 for data).

The nonequilibrium kinetic model accurately described breakthrough curves for Kr and SF_6 in partially saturated conditions (exp. 2−6). As described above, R and ω were used as fitting parameters for modeling the Kr and SF_6 breakthrough curves; V_g/V_w and α were calculated based on eqs 4 and 7d. The values for R estimated using mass balance (eq 2, Figure 3B,C) compared favorably in most cases with the values estimated from the model. However, when C/C_0 in the tracer breakthrough did not reach unity, R was underestimated (an inherent limitation of this method). This effect is clearly observed for SF_6 in exps. 2 and 3.

The Kr and SF_6 tracers were consistent in their estimates of V_g/V_w as established by the nearly 1:1 correlation between the values estimated from the Kr and SF_6 breakthrough curves (Figure 5A). Data from exp. 3 was not included in this analysis because of sampling error. In most experiments, estimates of V_g/V_w from fitted Kr and SF_6 breakthrough curves were similar to the gravimetrically measured values at the end of the experiment (Table 3, Figure 3B,C). It can be concluded there is good agreement between V_g/V_w values individually estimated from SF_6 and Kr retardation and the gravimetrically measured final value of V_g/V_w (p-values $\leq$0.05 for 95% confidence interval, Figure 5B). It can further be concluded that R values for one gas can be accurately predicted from the model-estimated R and V_g/V_w value of the other gas.

3.3. Influence of Flow Velocity. Partitioning behavior of dissolved gases is also influenced by tracer residence time (eq 6). Hence, the longer the residence time of the tracer in the column, the more time the tracer has to equilibrate with the surrounding medium (e.g., gas-filled void space). Diffusion constants for dissolved gases are typically much larger in air than in water (*45*). In addition, aqueous diffusion

coefficients differ among tracers (e.g., the value for SF_6 is ~65% and 70% that of Kr in water and air, respectively, Table 1). Based on various gas−water exchange model theories, the diffusion of Kr is greater than that of SF_6 at the gas−water interface (*35*).

The presence of gas-filled void space in the column can create a nonuniform flow-field resulting in an asymmetrical breakthrough curve for a partitioning tracer (e.g., Figure 4). This phenomenon is analogous to the presence of "immobile" water in a column where the retention and release of the tracer is mediated by diffusive mass transfer between the mobile and immobile phases (*46*). In the case of our two-phase system (water and air), the gas-filled void space is analogous to immobile water in that dissolved gases diffuse in and out of the region depending on the physicochemical conditions, resulting in asymmetric breakthrough curves (*42*). A similar effect has been previously observed when nonreactive tracers having different aqueous diffusion rates were injected into groundwater media containing intragranular pore spaces (*15*, *33*). Increased flow velocity magnifies this effect as the gas with lower interfacial diffusion rate requires a longer residence time to reach equilibrium between the phases.

Three experiments were performed to gauge this effect by injecting long pulses of the tracer solution into columns at similar values of V_g/V_w but different flow velocities. For similar V_g/V_w values, R should remain unaffected according to eq 4 for either gas regardless of flow velocity. The shapes of the resulting breakthrough curves were strongly influenced by flow velocity, while the retardation factors for both Kr and SF_6 remained similar (Figure 4 and Tables 2 and 3). The breakthrough curves appeared more symmetric at lower velocities, especially in case of SF_6. As flow velocity increased, the breakthrough curves became increasingly asymmetric, indicating that the partitioning behavior was strongly affected by the time of contact between the dissolved gas and the gas-filled void space. As described above, this asymmetry was caused by rate-limited partitioning of gases from the aqueous phase into the gaseous phase. This partitioning is described by the first-order rate coefficient, α (eqs 6), that is directly related to the flow velocity, ν_w, and inversely related to V_g/V_w (cf. eqs 4 and 7d). Therefore, any dissolved gas that exhibits a strong correlation between α and ν_w partitions more rapidly from the aqueous phase to the gas phase as the flow velocity increases.

In addition to the time of contact, the mass transfer of the gases across the gas−water interface is also directly related to the thickness of the water layer surrounding the air pockets. Assuming that all physical conditions in the column remain constant (size and shape of gas pockets), gases that diffuse at a higher rate through water reach the gas−water interface sooner thereby reaching equilibrium at the interface more rapidly. The aqueous diffusion coefficient for SF_6 is lower than that of Kr and hence there is greater asymmetry observed for SF_6 breakthrough curves as ν_w is increased.

The first-order rate coefficient, α, was estimated from the model fits of all breakthrough curves and plotted against ν_w in Figure 6 (see Table 2 for data). A strong linear correlation existed between α and ν_w ($r^2 = 0.99$ and 0.96 for Kr and SF_6, respectively). The slope of the relationship for Kr (~0.055) was approximately 1 order of magnitude greater than that for SF_6 (~0.005), implying that the mass transfer rate for dissolved SF_6 between the aqueous and gaseous phase was much lower than that for Kr. Therefore, when compared to SF_6, instantaneous equilibrium was attained between the aqueous and gaseous phases for Kr. In contrast, no such equilibrium existed for SF_6 in any experiment with $V_g/V_w > 0$, resulting in the increased asymmetry in breakthrough with an increased flow velocity (Figure 4).

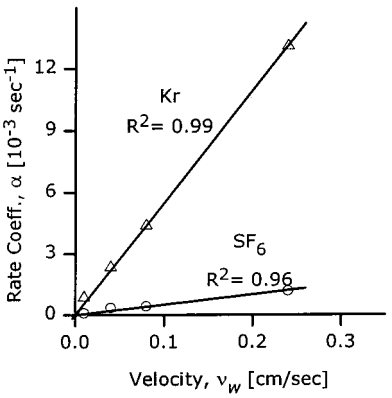

FIGURE 6. Linear correlation between the rate coefficient, α, and the flow velocity, nw, for dissolved SF_6 (○) and Kr (△). See Table 2 for data.

Various exchange models, based on a priori assumptions regarding exchange of gases across boundary layers, can be invoked to gain mechanistic insights into the gas exchange at the interface (*35*, *45*). In the case of a "Stagnant Two-Film Model" (*47*), where two stagnant layers exist adjacent to the gas−water interface, gas molecules must diffuse across both layers. According to Fick's first law of diffusion, the molecular flux F ($ML^{-2}\ T^{-1}$) is directly related to the concentration C (ML^{-3}) gradient across each layer and inversely related to the thickness of that layer z (L)

$$F = -D_m \frac{\partial C}{\partial z} \tag{8}$$

where D_m (L^2T^{-1}) is the molecular diffusion coefficient for the gas in the stagnant layer. At steady-state, these fluxes become equal giving rise to an overall mass transfer coefficient or velocity (D_m/z, LT^{-1}), which in the two-film model reflects the combined effects of gas molecules diffusing through two stagnant layers in series. In our case, D_m for Kr in both air and water is greater than that for SF_6, primarily due to smaller molecular mass and molar volume (volume/mole of gas) of the former species (*35*). Therefore, Kr diffuses across the stagnant layers faster than SF_6. In addition, the thickness of these layers is affected by shear stress on the gas−water boundary due to advection. In the case of aqueous transport, as water velocity increases, the boundary layer thickness decreases resulting in greater mass transfer across the liquid−gas interface. In this situation, the rate coefficient α should increase with velocity as was observed in Figure 6.

The information obtained from the breakthrough curves for these dissolved gas tracers can also be used to estimate interfacial area. Donaldson et al. (*36*) explicitly included interfacial area in the expression for mass transfer (eq 6), resulting in a slightly different transport equation (eq 7). However, they were unable to verify the estimated interfacial areas with an independent technique. Interfacial tracers that only partition at gas−water interface are required to estimate such parameters (*48*). In all cases, the combination of partitioning and nonpartitioning tracers, such as the ones used in this study, are required to accurately characterize partially water-saturated media.

The present study suggests SF_6 will be more responsive compared to Kr to the presence of nonaqueous phases in groundwater porous media (*14*, *32*, *49*, *50*). However, large tails in the breakthrough curves can be expected due to slow diffusion in to and out of dead end pore spaces, gas-filled void space, and/or diffusion into organic phases (*19*, *33*). This behavior can help in understanding factors affecting removal of volatile organic compounds commonly found in contaminated groundwaters.

Injection of a combination of dissolved gases that differ substantially in their physical properties (e.g., K_H and D_m) may help in better characterization as demonstrated in this laboratory study. Despite higher initial cost for obtaining noble gases, extremely low detection limits and background levels of most noble gases require that only an extremely small amount be used in comparison to conventional solutes.

Acknowledgments

The authors thank Dr. Gary Mills and Susan Hayden of SREL for laboratory assistance. We also thank Dr. Randy Culp of Center for Applied Isotope Studies, the University of Georgia, Athens, GA for introducing us to the use of dissolved gases as tracers and Dr. David Dunn of SRTC, Westinghouse Savannah River Company, Savannah River Site, Aiken, SC for guidance on potential field applications. Financial assistance was provided through Financial Assistance Award number DE-FC09-96SR18546 from the U.S. Department of Energy to the University of Georgia Research Foundation.

Literature Cited

(1) Benson, C. F.; Bowman, R. S. *Soil Sci. Soc. Am. J.* **1994**, *58*, 1123−1129.
(2) Jaynes, D. B. *Ground Water* **1994**, *32*(*4*), 532−538.
(3) Bowman, R. S.; Gibbens, J. F. *Ground Water* **1992**, *30*(*1*), 8−14.
(4) Boggs, M. J.; Adams, E. E. *Water Resour. Res.* **1992**, *28*(*12*), 3325−3336.
(5) Bertsch, P. M.; Seaman, J. C. *Proc. Natl. Acad. Sci. U.S.A.* **1999**, *96*, 3350- 3357.
(6) Seaman, J. C. *Soil Sci. Soc. Am. J.* **1998**, *62*, 354−361.
(7) Seaman, J. C.; Bertsch, P. M.; Strom, R. N. *Environ. Sci. Technol.* **1997**, *31*, 2782−2790.
(8) Seaman, J. C.; Bertsch, P. M.; Miller, W. P. *J. Contam. Hydrol.* **1995**, *20*, 127−143.
(9) Ishiguro, M.; Song, K.; Yuite, K. *Soil Sci. Soc. Am. J.* **1992**, *56*, 1789−1793.
(10) Ryan, J. N.;Gschwend, P. M. *Water Resour. Res.* **1990**, *26*(*2*), 307−322.
(11) Chan, K.; Geering, H.; Davey, B. *J. Environ. Qual.* **1980**, *9*, 579−582.
(12) Seaman, J. C.; Bertsch, P. M.; Korom, S. F.; Miller, W. P. *Ground Water* **1996**, *34*(*5*), 778−783.
(13) Jones, B. W. M.S. Thesis, The University of Georgia, 1996.
(14) Nelson, N. T.; Brusseau, M. L. *Environ. Sci. Technol.* **1996**, *30*, 2859−2863.
(15) Sanford, W. E.; Shropshire, R. G.; Solomon, D. K. *Water Resour. Res.* **1996**, *32*(*6*), 1635−1642.
(16) Wilson, R. D.; Mackay, D. M. *Ground Water* **1996**, *34*, 241−249.
(17) Fry, V. A.; Istok, J. D.; Semprini, L.; O'Reilly, K. T.; Buscheck, T. E. *Ground Water* **1995**, *33*(*3*), 391−398.
(18) Olschewski, A.; Fischer, U.; Hofer, M. *Environ. Sci. Technol.* **1995**, *29*, 264−266.
(19) Upstill-Goddard, R. C.; Wilkins, C. S. *Water Res.* **1995**, *29*, 1065−1068.
(20) Carter, R. C.; Kaufman, W. J.; Orlob, G. T.; Todd, D. K. *J. Geophys. Res.* **1959**, *64*, 2433−2439.
(21) Hibbs, D. E.; Parkhill, K. L.; Gulliver, J. S. *J. Environ. Eng.* **1998**, *124*, 752−760.
(22) Ho, D. T.; Schlosser, P.; Smethie, W. M., Jr.; Simpson, H. J. *Environ. Sci. Technol.* **1998**, *32*, 2377−2382.
(23) Szabo, Z.; Rice, D. E.; Plummer, L. N.; Busenberg, E.; Drenkard, S.; Schlosser, P. *Water Resour. Res.* **1996**, *32*, 1023−1038.
(24) Ekwurzel, B.; Schlosser, P.; Smethie, W. M., Jr.; Plummer, L. N.; Busenberg, E.; Michel, R. L.; Weppernig, R.; Stute, M. *Water Resour. Res.* **1994**, *30*, 1693−1708.
(25) Dunkle, S. A.; Plummer, L. N.; Busenberg, E.; Phillips, P. J.; Denver, J. M.;Hamilton, P. A.; Michel, R. L.; Coplen, T. B. *Water Resour. Res.* **1993**, *29*, 3837−3860.
(26) Busenberg, E.; Plummer, L. N. *Water Resour. Res.* **2000**, *36*, 3011−3030.
(27) Maiss, M.; Steele, L. P.; Francey, R. J. *Atmos. Environ.* **1996**, *30*, 1621−1629.
(28) Davis, S. N.; Campbell, D. J.; Bentley, H. W.; Flynn, T. J. Groundwater tracers; Technical report; R. S. Kerr Environmental Research Lab, U.S. Environmental Protection Agency: 1985.
(29) Wanninkhof, R.; Ledwell, J. R.; Watson, A. J. *J. Geophys. Res.* **1991**, *96*, 8733−8740.
(30) Galdiga, C. U.; Greibrokk, T. *Chromatographia* **1997**, *46*, 440−443.
(31) Wilson, R. D.; Mackay, D. M. *Ground Water* **1993**, *31*, 719−724.
(32) Wilson, R. D.; Mackay, D. M. *Environ. Sci. Technol.* **1995**, *29*, 1255−1258.
(33) Jardine, P. M.; Sanford, W. E.; Gwo, J. P.; Reedy, O. C.; Hicks, D.S.; Riggs, J. S.; Bailey, W. B. *Water Resour. Res.* **1999**, *35*, 2015−2030.
(34) Smethie, W. M.; Solomon, D. K.; Schiff, S. L.; Mathieu, G. G. *J. Hydrol.* **1992**, *130*(*1*), 279−297.
(35) Schwarzenbach, R. P.; Gschwend, P. M.; Imboden, D. M. *Environmental organic chemistry;* Wiley: New York, 1993.
(36) Donaldson, J. H.; Istok, J. D.; Humphrey, M. D.; O'Reilly, K. T.; Hawelka, C. A.; Mohr, D. H. *Ground Water* **1997**, *35*(*2*), 270−279.
(37) van Genuchten, M. T. *Nonequilibrium transport parameters from miscible displacement experiments*; Research Report 119; U.S. Department of Agriculture, U.S. Salinity Lab.: 1981.
(38) NCASI. *Development of a gas chromatagraphic protocol for the measurement of krypton gas in water and demonstration of its use in stream reaeration measurements*; Technical Report SERIES: Technical bulletin no. 614; National Council of the Paper Industry for Air and Stream Improvement: 1991.
(39) Wanninkhof, R.; Mullholland, P. J.; Elwood, J. W. *Water Resour. Res.* **1990**, *26*, 1621−1630.
(40) Nkedi-Kizza, P.; Rao, P. S. C.; Hornsby, A. S. *Environ. Sci. Technol.* **1987**, *21*, 1107−1111.
(41) Yu, C.; Warrick, A. W.; Conklin, M. H. *Water Resour. Res.* **1999**, *35*, 3567−3572.
(42) Brusseau, M. L. In *Physical nonequilibrium in soils: Modeling and application*; Selim, H. M., Ma, L., Eds.; Ann Arbor Press: Chelsea, MI, 1998; pp 63−82.
(43) Leij, F. J.; Toride, N. In *Physical nonequilibrium in soils: Modeling and application*; Selim, H. M., Ma, L., Eds.; Ann Arbor Press: Chelsea, MI, 1998; pp 117−156.
(44) van Genuchten, M. T.; Alves, W. J. *Analytical solutions of the one-dimensional and convective-dispersive solute transport equation*; Technical Bulletin 1661; U.S. Department of Agriculture, U.S. Salinity Lab.: 1982.
(45) Cussler, E. L. *Diffusion: Mass transfer in fluid systems*, 2nd ed.; Cambridge University Press: Cambridge, U.K., 1997.
(46) Brusseau, M. L. *Water Resour. Res.* **1993**, *29*, 1071−1080.
(47) Liss, P. S.; Slater, P. G. *Nature* **1974**, *247*, 181−184.
(48) Kim, H.; Rao, P. S. C.; Annable, M. C. *Soil Sci. Soc. Am. J.* **1999**, *63*, 1554−1560.
(49) Jin, M.; Delshad, M.; Dwarakanath, V.; McKinney, D. C.; Pope, G. A.; Sepehnoori, K.; Tilburg, C. *Water Resour. Res.* **1995**, *31*, 1201−1216.
(50) Young, C. M.; Jackson, R. E.; Jin, M.; Londergan, J. T.; Mariner, P. E.; Pope,G. A.; Anderson, F. J.; Houk, T. *Ground Water Monitor. Remed.* **1999**, *19*(*1*), 84−94.
(51) Wilhelm, E.; Battino, R.; Wilcock, R. J. *Chem. Rev.* **1977**, *77*, 219−262.
(52) Jahne, B.; Heinz, G.; Dietrich, W. *J. Geophys. Res.* **1987**, *92*, 767−776.
(53) Butler, J. H.; Battle, M.; Bender, M. L.; Montzka, S. A.; Clarke, A. D.; Saltzman,E. S.; Sucher, C. M.; Severinghaus, J. P.; Elkins, J. W. *Nature* **1999**, *399*, 749−755.
(54) Gluekauf, E.; Kitt, G. P. *Proc. Royal Soc. London* **1956**, *234*, 557−565.

Received for review March 5, 2001. Revised manuscript received August 23, 2001. Accepted September 18, 2001.

ES0107024